

Microscopic Enhancement of Heavy-Element Production

P. Möller¹ and J. R. Nix

Theoretical Division, Los Alamos National Laboratory, Los Alamos, NM 87545, USA

P. Armbruster, S. Hofmann, and G. Münzenberg

Gesellschaft für Schwerionenforschung, Planckstrasse 1, D64291 Darmstadt, Germany

April 4, 1997

Abstract. Realistic fusion barriers are calculated in a macroscopic-microscopic model for several soft-fusion heavy-ion reactions leading to heavy and superheavy elements. The results obtained in such a realistic picture are very different from those obtained in a purely macroscopic model. For reactions on ^{208}Pb targets, shell effects in the entrance channel result in fusion-barrier energies at the touching point that are only a few MeV higher than the ground state for compound systems near $Z = 110$. The entrance-channel fragment-shell effects remain far inside the touching point, almost to configurations only slightly more elongated than the ground-state configuration, where the fusion barrier has risen to about 10 MeV above the ground-state energy. Calculated single-particle level diagrams show that few level crossings occur until the peak in the fusion barrier very close to the ground-state shape is reached, which indicates that dissipation is negligible until very late in the fusion process. Whereas the fission valley in a macroscopic picture is several tens of MeV lower in energy than is the fusion valley, we find in the macroscopic-microscopic picture that the fission valley is only about 5 MeV lower than the fusion valley for soft-fusion reactions leading to compound systems near $Z = 110$. These results show that no significant “extra-extra-push” energy is needed to bring the system inside the fission saddle point and that the typical reaction energies for maximum cross section in heavy-element synthesis correspond to only a few MeV above the maximum in the fusion barrier.

1 Introduction

Cross sections for complete fusion in heavy-ion reactions vary predictably and smoothly from the lightest compound systems up to compound systems with nucleon number about $A = 200$. Beyond $A = 200$, the compound-nucleus cross sections drop dramatically [1–3]. A multi-dimensional macroscopic dynamical model that explores a sufficiently general deformation space to allow two touching spheres in the entrance channel to evolve towards a single spherical shape *and* towards fission configurations provides an explanation of the mechanism behind the sudden drop in cross sections for heavy compound-nucleus formation [4–7].

For light projectiles and targets leading to compound systems below $A = 200$, the fusion and fission valleys are roughly equivalent and the fission saddle point is more elongated than two touching spheres. As the nucleon number A increases above 200 the fission saddle-point shape rapidly becomes less elongated and recedes to a more compact shape than the fusion touching configuration. At the touching configuration for these heavy nuclei, the steepest slope of the potential-energy surface is towards the fission valley *outside* the fission saddle point. Thus, if two

¹ Permanent address: *P. Möller Scientific Computing and Graphics, Inc., P. O. Box 1440, Los Alamos, New Mexico 87544, USA*

colliding ions are brought together with just enough energy to reach the touching configuration, the system will evolve towards the fission valley and reseparate without forming a compound system. A *necessary* condition [4,5] for forming a compound system is that the dynamical trajectory evolves to shapes inside the fission saddle point, that is, to shapes between the spherical or deformed ground-state shape and the fission saddle point. In a dynamical macroscopic model this can only be accomplished by bringing the colliding heavy ions together with energies substantially above the energy of the touching configuration. The energy has to be higher both because the maximum of the static fusion barrier is located somewhat inside the touching point for heavy systems and because in a multi-dimensional deformation space the topography of the potential is such that the trajectory is deflected towards points outside the fission saddle point. For collisions leading to nuclei between the actinides and the superheavy elements it is the dynamical deflection of the trajectory that is the most important effect. The extra energy above the maximum in the fusion barrier that is required to prevent deflection of the fusion trajectory to the fission valley is often referred to as the “extra-extra-push” energy [8,9]. The results of such macroscopic dynamical calculations indicate that for complete fusion leading to heavy elements in the region $Z = 100$ – 110 the optimum reaction energy is several tens of MeV above the energy of the touching configuration.

Some reaction cross sections agree with this anticipated dependence on the reaction energy, but most reactions cannot be even qualitatively understood in terms of such a macroscopic model. Particularly notable exceptions have been observed in the synthesis of the six elements with proton number $Z = 107$ – 112 [10–15] in soft-fusion reactions on targets near ^{208}Pb . In these reactions the optimum cross sections are obtained below the macroscopic one-dimensional Bass model of the fusion barrier [16,17]. The optimum cross sections are obtained at energies 8–4 MeV below the Bass barrier, corresponding to 14–10 MeV excitation energy in the compound system. Thus, the cross sections for these reactions cannot be understood in terms of existing macroscopic models.

The soft-fusion reaction has long been thought to enhance heavy-element evaporation-residue cross sections primarily because it leads to compound nuclei of low excitation energy, which enhances de-excitation by neutron emission relative to fission. Higher excitation energies would lead to higher fission probabilities. However, the evaporation-residue cross section is the product of the cross section for compound-nucleus formation and the probability for de-excitation by neutron emission. One may therefore ask if soft fusion *also* enhances the cross section for compound-nucleus formation. Because of the low excitation energies in the entrance channel, the large negative shell correction associated with target nuclei near the doubly magic ^{208}Pb should be almost fully manifested at touching and slightly inside touching.

Nuclei near ^{258}Fm have already provided important insight into fragment shell effects in symmetric fission and fusion configurations [18–20]. At ^{258}Fm fission becomes symmetric with a very narrow mass distribution, the kinetic energy of the fragments is about 35 MeV higher than in the asymmetric fission of ^{256}Fm and the spontaneous-fission half-life is 0.38 ms for ^{258}Fm compared to 2.86 h for ^{256}Fm . These features are well understood in terms of the macroscopic-microscopic model. Shell effects associated with division into fragments near ^{132}Sn lower the fusion valley at touching by about -20 MeV in the most favorable case, relative to a macroscopic potential-energy model. This fragment shell effect remains important far inside the touching point and results in fission into the fusion valley with very compact *cold* fragments for several fissioning nuclei in the vicinity of ^{258}Fm . Calculated single-particle level diagrams and potential-energy surfaces show that these fragment shell effects start to become important already slightly outside the first saddle in the potential-energy surface. We now show that shell effects are also very important in the fusion entrance channel in soft-fusion heavy-ion reactions, which usually involve *asymmetric* projectile-target combinations.

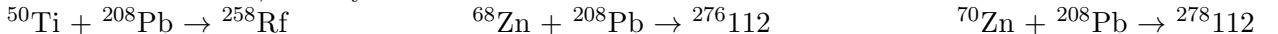
2 The soft-fusion entrance channel

Our calculations here of single-particle level diagrams and potential energies are based on the finite-range droplet model in its 1992 version [FRDM (1992)]. In this macroscopic-microscopic model we use a generalized droplet model with a Yukawa-plus-exponential term for the nuclear energy as the macroscopic model and a realistic, diffuse-surface folded-Yukawa single-particle potential as the starting point for calculating the microscopic term by use of Strutinsky's method. Special care has been taken to formulate the model so that the same energy is obtained for the touching-sphere configuration both when this configuration is considered as one highly deformed nucleus and when it is considered as two separate nuclei with macroscopic and microscopic interactions. The requirement that the energy be the same in these two cases has led to the incorporation of shape-dependent Wigner and pairing energies in the model and to a shape-dependent smoothing range in the Strutinsky shell-correction method [19]. Complete details can be found in Ref. [21].

For the symmetric fusion of two ^{132}Sn nuclei the minimum-energy configuration for the two merging ions corresponds to two intersecting spheres for a substantial part of the trajectory from the touching point to the single sphere [20]. In our study here of the asymmetric soft-fusion reactions we therefore select intersecting spheres as our fusion shape configurations. As the deformation coordinate we use r , the distance between the centers of mass of the two intersecting spheres. These centers of mass coincide with the centers of the spheres *only* for the touching configuration.

In Figs. 1 and 2 we show calculated proton and neutron single-particle level diagrams for this sequence of shapes in terms of the r shape coordinate for the reaction $^{70}\text{Zn} + ^{208}\text{Pb} \rightarrow ^{278}112$. This represents the reaction employed to reach the heaviest nucleus known thus far. In the proton single-particle level diagram in Fig. 1 the magic-fragment gap combination $28 + 82 = 110$ remains far inside the touching point, up to about $r/R_0 = 1.15$. The quantity R_0 is the radius of the spherical compound system. This is in excellent agreement with the results of calculations related to the symmetric fission of nuclei near ^{258}Fm into symmetric spherical fragments near ^{132}Sn . In the neutron single-particle level diagram in Fig. 2 the magic-fragment gap combination $40 + 126 = 166$ is less prominent. However, since the level density is low both above and below this neutron number the resulting microscopic correction will also be low. This region of relatively low single-particle level density also remains for a substantial distance inside the touching point, up to about $r/R_0 = 1.15$.

To quantitatively study the effect of the persistent magic-fragment gaps on the fusion barrier as the heavy ions merge we have calculated the fusion barrier for intersecting spheres for three reactions of interest, namely:



which are shown in Figs. 3–5, respectively. Just beyond the peak in the fusion barrier at about $r/R_0 = 1.0$ we have switched from the intersecting-sphere parameterization to Nilsson's perturbed spheroid ϵ parameterization so that we accurately obtain the energy of the ground state. The calculated ground-state shapes are indicated in the figures. For each reaction we also show the touching configurations and one intersecting-sphere configuration at $r/R_0 = 1.04$, just before the maximum in the fusion barrier. The dotted line shows the calculated fission barrier, for which we considered only ϵ_2 and ϵ_4 shape distortions. The effect of mass asymmetry on the fission barrier is expected to be small for the two heavier nuclei, but up to 2 MeV for the ^{258}Rf barrier at distortions larger than about $r/R_0 = 1.3$ [22]. The fusion barrier in the macroscopic FRDM without any shell effects is given by the short-dashed line. The touching configuration in all three cases is indicated by a thin vertical long-dashed line. For the reactions in Figs. 3 and 5 the arrow indicates the incident energy corresponding to the maximum evaporation-residue cross section.

3 Discussion

Clearly, the inclusion of microscopic effects in the calculation of the fusion barrier has major consequences. Whereas the incident energy corresponding to a maximum 1n evaporation-residue cross section is far below a macroscopic barrier [16,17], it is at or slightly above the maximum in our realistic fusion barrier. The maximum occurs at about $r/R_0 = 1.0$, where our overlapping-sphere configuration may not be general enough for an accurate calculation. From comparisons with multi-dimensional calculations in the Fm region we conclude that exploring a more general multi-dimensional parameterization may in some cases lower the maximum fusion barrier by 2 or 3 MeV. Thus, the incident energy is slightly above the maximum of a still more realistic fusion barrier.

It has been argued earlier that shell effects in the soft-fusion entrance channel favor compound-nucleus formation both because they lower the fusion barrier, so that fusion is possible at lower energies [5,7,23], and because the persistence of the fusion valley far inside the touching point prevents deflection towards the fission valley [18].

It is also of interest to understand how some of the kinetic energy in the soft-fusion entrance channel is dissipated into internal energy. If the dissipation occurs early in the fusion process then extra energy over and above the fusion barrier would be needed to push the system inside the saddle point. However, it was argued earlier [3,24] that level diagrams for fission/fusion of ^{264}Fm showed few level crossings occurring in the merging of two ^{132}Sn nuclei between touching and about $r/R_0 = 1.15$ and in analogy the situation in soft fusion on ^{208}Pb targets should be similar. In that case, little dissipation would occur until just outside the inner fusion and fission saddle points, which would again reduce significantly the need for extra energy in the entrance channel to reach the compound-nucleus configuration inside the fission saddle point.

We see here in Figs. 1 and 2 that the analogy postulated in Ref. [3,24] is borne out. The first crossings near the Fermi surface do not occur until about $r/R_0 = 1.15$ for protons. For neutrons, although the $N = 166$ gap disappears for larger values of r , the low level density associated with this neutron number also persists until about $r/R_0 = 1.15$. However, the large majority of level crossings occur at $r/R_0 = 1.0$ or even inside, that is, right at the peak of the fusion and fission barrier, very close to the ground-state shape. This means that the original fragment “cluster” or shell structure is preserved during most of the fusion process. This preservation of the original incident fragment structure is also qualitatively clear from the appearance of the intersecting-sphere shape at $r/R_0 = 1.04$ in Figs. 3–5. This preservation of fragment character is maintained even further inside the touching point than argued and very schematically indicated in Fig. 18 of Ref. [3].

Our present macroscopic-microscopic calculations provide a much improved understanding of the soft-fusion process, relative to a macroscopic-only multi-dimensional picture [4–7] and relative to the one-dimensional Bass model [16,17], which are both clearly insufficient to provide an interpretation of the soft-fusion process. A microscopic picture results in completely different fusion barriers, potential-landscape valley structures, and dissipation mechanisms. In addition, the dissipation depends critically on the evolution of the fusion trajectory and on the system location on this trajectory. The major part of the dissipation takes place very near ground-state shape configurations.

4 Conclusions

The results here are the first step in a completely new and more complete picture of soft fusion, a picture that has the potential of eventually providing a more quantitative model of the magnitude and the location in energy of the $1n$ evaporation-residue cross section. The results here already show that the maximum cross section occurs a few MeV above a *realistic* fusion barrier. Our results also show that the differences in the magnitude of the $1n$ evaporation-residue cross section can be interpreted in terms of a microscopic dissipation process at the inner fusion/fission barrier and the dynamics of the fusion trajectory, which, just as in the macroscopic picture, is located higher in energy than is the fission valley. However, the fusion entrance channel is only 5 MeV or so higher than the fission valley in the initial stage of fusion and the difference is even smaller later, in contrast to several tens of MeV differences in a macroscopic-only picture. An emission of a pre-compound neutron inside a realistic fusion barrier would cool the compound system to an excitation energy that is below the fission barrier. For further understanding of the soft-fusion evaporation-residue cross section, multi-dimensional calculations of the fusion/fission landscape are required. Dynamical studies, properly incorporating a microscopic dissipation model, of the trajectory in this potential-energy landscape should provide additional insight.

This work was supported by the U. S. Department of Energy.

References

- 1) P. Armbruster, Ann. Rev. Nucl. Part. Sci. **35** (1985) 135.
- 2) G. Münzenberg, Rep. Prog. Phys. **51** (1988) 57.
- 3) P. Armbruster, J. Phys. Soc. Jpn. **58** Suppl. (1989) 232.
- 4) A. J. Sierk and J. R. Nix, Proc. Third IAEA Symp. on the physics and chemistry of fission, Rochester, New York, 1973, vol. II (IAEA, Vienna, 1974) 273.
- 5) J. R. Nix and A. J. Sierk, Phys. Scr. **10A** (1974) 94.
- 6) P. Möller and J. R. Nix, Nucl. Phys. **A272** (1976) 502.
- 7) P. Möller and J. R. Nix, Nucl. Phys. **A281** (1977) 354.
- 8) W. J. Swiatecki, Phys. Scr. **24** (1981) 113.
- 9) W. J. Swiatecki, Nucl. Phys. **A376** (1982) 275.
- 10) G. Münzenberg, S. Hofmann, F. P. Heßberger, W. Reisdorf, K.-H. Schmidt, J. R. H. Schneider, P. Armbruster, C.-C. Sahm, and B. Thuma, Z. Phys. **A300** (1981) 7.
- 11) G. Münzenberg, P. Armbruster, F. P. Heßberger, S. Hofmann, K. Poppensieker, W. Reisdorf, J. R. H. Schneider, W. F. W. Schneider, K.-H. Schmidt, C.-C. Sahm, and D. Vermeulen, Z. Phys. **A309** (1982) 89.
- 12) G. Münzenberg, P. Armbruster, H. Folger, F. P. Heßberger, S. Hofmann, J. Keller, K. Poppensieker, W. Reisdorf, K.-H. Schmidt, H. J. Schött, M. E. Leino, and R. Hingmann, Z. Phys. **A317** (1984) 235.
- 13) S. Hofmann, N. Ninov, F. P. Heßberger, P. Armbruster, H. Folger, G. Münzenberg, H. J. Schött, A. G. Popeko, A. V. Yeremin, A. N. Andreyev, S. Saro, R. Janik, and M. Leino, Z. Phys. **A350** (1995) 277.
- 14) S. Hofmann, N. Ninov, F. P. Heßberger, P. Armbruster, H. Folger, G. Münzenberg, H. J. Schött, A. G. Popeko, A. V. Yeremin, A. N. Andreyev, S. Saro, R. Janik, and M. Leino, Z. Phys. **A350** (1995) 281.
- 15) S. Hofmann, N. Ninov, F. P. Heßberger, P. Armbruster, H. Folger, G. Münzenberg, H. J. Schött, A. G. Popeko, A. V. Yeremin, S. Saro, R. Janik, and M. Leino, Z. Phys. **A354** (1996) 229.
- 16) R. Bass, Phys. Lett. **47B** (1973) 139.
- 17) R. Bass, Nucl. Phys. **A231** (1974) 45.
- 18) P. Möller, J. R. Nix, and W. J. Swiatecki, Nucl. Phys. **A469** (1987) 1.
- 19) P. Möller, J. R. Nix, and W. J. Swiatecki, Nucl. Phys. **A492** (1989) 349.
- 20) P. Möller and J. R. Nix, J. Phys. G: Nucl. Part. Phys. **20** (1994) 1681.
- 21) P. Möller, J. R. Nix, W. D. Myers, and W. J. Swiatecki, Atomic Data Nucl. Data Tables **59** (1995) 185.
- 22) P. Möller and J. R. Nix, Nucl. Phys. **A229** (1974) 269.
- 23) A. Săndulescu, R. K. Gupta, W. Scheid, and W. Greiner, Phys. Lett. **60B** (1976) 225.
- 24) P. Armbruster, Proc. Int. School-Seminar on Heavy Ion Physics, Dubna, Russia, 1986, Joint Institute for Nuclear Research Report No. D7-87-68 (1987) 82.

Figure captions

- Fig. 1 Proton single-particle level diagram for merging nuclei in an asymmetric heavy-ion collision leading to the heaviest known nucleus. The asymmetric configuration in the entrance channel leads to a mixing of states with odd and even parity. The magic-fragment gaps associated with the initial entrance-channel configuration remain far inside the touching point, to about $r/R_0 = 1.15$, somewhat outside the maximum in the fusion barrier.
- Fig. 2 Neutron single-particle level diagram for merging nuclei in an asymmetric heavy-ion collision leading to the heaviest known nucleus. The asymmetric configuration in the entrance channel leads to a mixing of states with odd and even parity.
- Fig. 3 Total and macroscopic fusion barriers for the soft-fusion reaction $^{50}\text{Ti} + ^{208}\text{Pb} \rightarrow ^{258}\text{Rf}$ and fission barrier corresponding to spontaneous fission from the ground state.
- Fig. 4 Total and macroscopic fusion barriers for the soft-fusion reaction $^{68}\text{Zn} + ^{208}\text{Pb} \rightarrow ^{276}112$ and fission barrier corresponding to spontaneous fission from the ground state.
- Fig. 5 Total and macroscopic fusion barriers for the soft-fusion reaction $^{70}\text{Zn} + ^{208}\text{Pb} \rightarrow ^{278}112$ and fission barrier corresponding to spontaneous fission from the ground state.